Imaging of Wrist Trauma

Nigel Raby

Contents

N. Raby (✉)
Department of Radiology, Westen Infirmary, Glasgow, G11 6NT, UK
e-mail: N.Raby@clinmed.gla.ac.uk; nigel.raby@ggc.scot.nhs.uk

Abstract

This chapter will principally describe and illustrate acute bony injuries of the distal radius and carpus occurring as a result of trauma. Plain films form the bulk of investigations, but where indicated use of CT and MR imaging is also included. Chronic traumatic injuries principally overuse, or stress injuries will also be considered but in less detail.

1 Introduction

1.1 Radiographic Anatomy and Projections

Standard radiographic views for the evaluation of wrist are a postero-antererior (PA) and lateral. These projections are described with the relevant anatomy in Radiography and Arthrography and will not be repeated here. These 2 views will allow evaluation of injuries of the distal radius and ulna, an assessment of the carpal bones, and the carpo-metacarpal junction. Additional views may be obtained in special specific circumstance most commonly when there is clinical suspicion of a scaphoid fracture.

1.2 Analysis of Radiographs

On the PA view, inspect each bone in turn looking for cortical disruption that would indicate a fracture. It is important to consider in turn the distal radius and ulna, then the eight carpal bones and finally the bases of the metacarpals. Next, undertake scrutiny of the normal uniform spacing of 1–2 mm around each carpal bone.

A. M. Davis et al. (eds.), *Imaging of the Hand and Wrist*, Medical Radiology. Diagnostic Imaging,
DOI: 10.1007/174_2010_110,

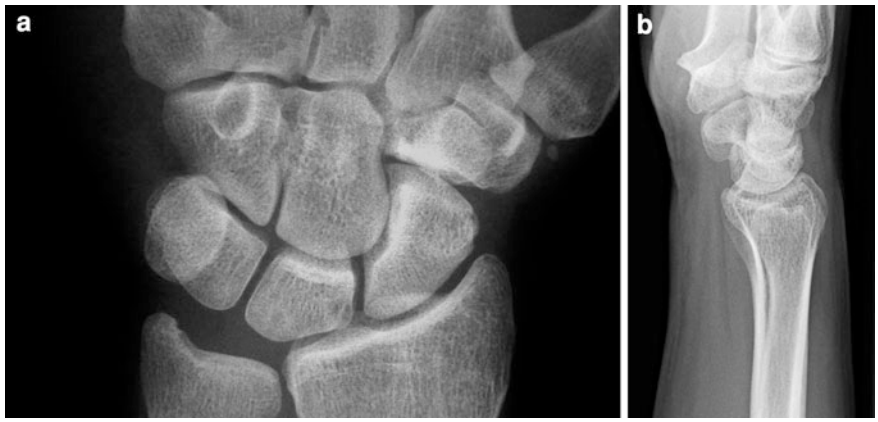

Fig. 1 **a** Normal AP radiograph. Note the uniform spacing between the carpal bones including the carpo-metacarpal junction. The 3 carpal arcs are smooth. The ulnar side of the 3rd metacarpal aligns with the space between the capitate and hamate. **b** Normal lateral radiograph. Observe the normal volar tilt of the distal radius. The dorsal cortex of the radius should be smooth with no steps or crinkles. Observe the normal alignment of the radius lunate and capitate

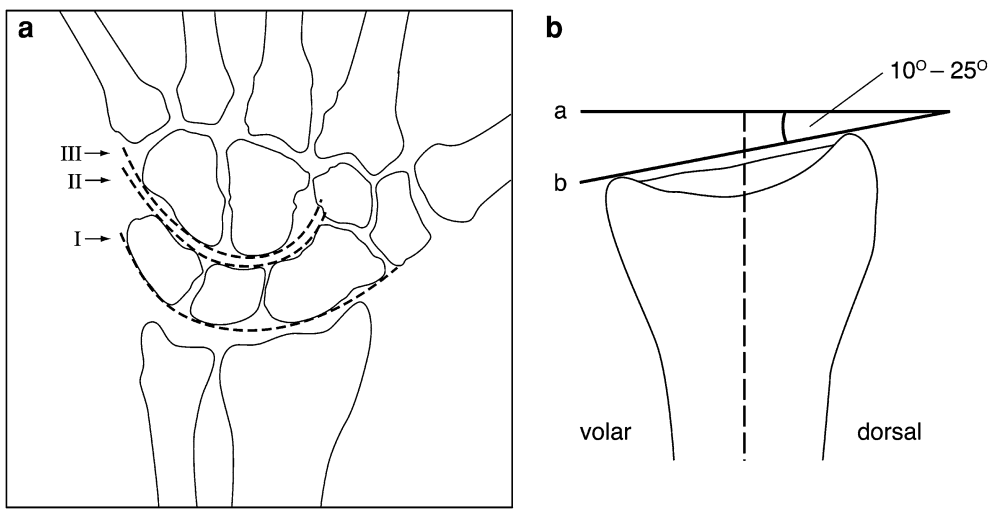

Fig. 2 **a** Line drawing indicating the position of the three carpal arcs. **b** The normal volar tilt of the distal radius

This spacing also occurs at the carpo-metcarpal junction. Loss of this spacing should lead to very careful inspection of the abnormal area, as often this will indicate significant carpal or carpo-metacarpal disruption (Fig. 1). One should also observe the arrangement of the carpal bones into smooth arcs. Three arcs have been described (Gilula 1979). The first delineates the proximal surface of the proximal row of carpal bones (scaphoid, lunate, triquetral). The second is formed by the distal articular surface of the same bones. The third is along the proximal curvature of the capitate and hamate (Fig. 2).

These arcs should normally be smooth with no steps or disruption. Interruption of any of these smooth arcs indicates a disruption of the normal arrangement of bony structures at the point of the step in the arc. Note should also be taken of the normal alignment of the metacarpals with the distal row of carpal bones, in particular, the relationship of the 3rd metacarpal with the distal capitate. A line drawn down the ulnar side of the metacarpal should pass through the joint between the capitate and hamate (Fig. 1). Loss of this normal alignment indicates a carpo-metacarpal disruption most commonly a dislocation. This sign is akin to the alignment of the tarsometatarsal joint in the foot.

Much important information is to be found on the lateral film. A key observation is that of the distal

radial angle. The normal distal radius has a volar tilt of approx 10°. This represents the angle between a line drawn along the long axis of the radius and a line drawn from the dorsal to the volar rim of the radius and has a normal range of 2°–20° (Figs. 1b, 2b). Alteration of this angle occurs when there is a subtle fracture of the distal radius. Normal relationship of the distal radius and carpal bones is best assessed on the lateral view, and this is discussed further in the Sect. 3.3. Displacement of the distal radial epiphysis and disruption of carpal alignment are often only evident on this view. Fractures of the triquetral bone will only be seen on the lateral radiograph.

CT is rarely used to confirm or refute the presence of a fracture. A fracture is usually evident on the plain films, but CT is helpful to define the exact anatomy in complex fractures and dislocations to aid surgical planning. This is particularly true when there is involvement of the articular surface of the radius such a Bartons fracture dislocation and die punch injuries. The exception is when an injury of isolated carpal bones is suspected. Fractures of these, particularly hamate and capitate, may be seen only on CT. CT is of value in some carpal dislocations but is particularly of value in cases of metacarpal dislocations which can be difficult to identify on plain films. In the current era of multislice scanners, there is no longer any need to be overly prescriptive about scan planes and slice thickness. Modern scanners allow very rapid multiplanar and 3D reconstruction with isotropic voxels, so that the injured wrist can be scanned in any position and reviewed in the best plane for the injury under investigation without any loss of information or degradation of the image.

MR is not generally utilised to evaluate acute wrist trauma, but it is the investigation of choice when an occult scaphoid fracture is suspected clinically.

1.3 Ligamentous Anatomy of Wrist

The ligamentous anatomy of the wrist is extremely complex. There is disagreement between authors with considerable variation in the description of the ligament anatomy. This anatomy has been dealt with in detail elsewhere in this book and will not be reiterated here. This level of understanding is important when evaluation of the ligaments by imaging is being undertaken. However, for the purposes of this chapter, such detail is not required. What is required is knowledge of important ligaments and their attachments. This information allows a better understanding of the patterns of bony injury and associated findings. Here, I will outline the key ligaments and indicate where in the later text this ligamentous knowledge applies. Of necessity, this is a much simplified account of the ligaments.

Ligaments are divided into extrinsic and intrinsic both dorsal and volar. The volar ligaments are stronger and more functionally significant. Extrinsic ligaments link the distal radius and ulna to the carpal bones. The intrinsic or intercarpal ligaments link carpal bones to one another.

On the dorsal aspect two ligaments are of importance in this chapter. They are the dorsal radiotriquetral (extrinsic) and the dorsal intercarpal ligament. Both attach to the triquetral bone. It is the attachment of these ligaments that account for the avulsion fracture of the triquetral (see below) (Fig. 3a).

On the volar aspect, there are 2 key ligaments. The radio scapho-capitate (RSC) and the radio lunate triquetral (RLT), both extrinsic ligaments (Fig. 3b). The position of the RSC helps understand the propensity of the scaphoid to fracture (see Sect. 3.1).

When the wrist is dorsiflexed, these two ligaments separate resulting in what is termed the space of Poirier. This space between the ligaments is an area of weakness which accounts for the carpal dislocations that occur around the lunate (see Sect. 3.3).

The attachments of the RSC and RLT to the radius account for the isolated fracture of the radial styloid which is essentially an avulsion injury. (See isolated fracture of radial styloid.)

In addition to the RSC and RLT, there are other ligaments that arise from the volar aspect of the radius to attach to carpal bones. Their names and arrangement are not important in this setting, but the multiple ligaments account for the bone fragments seen on the volar aspect of the wrist in patients with dorsal radio carpal dislocations (see Sect. 3.3).

On the ulnar aspect of the wrist lies the triangular fibrocartilage complex (TFCC). Again this has very complex anatomy, but for our purposes it is sufficient know that there are paired ligaments on dorsal and volar aspects of the wrist. The radio-ulnar ligaments pass horizontally between the radius and the ulna styloid process. There are also two ligaments running

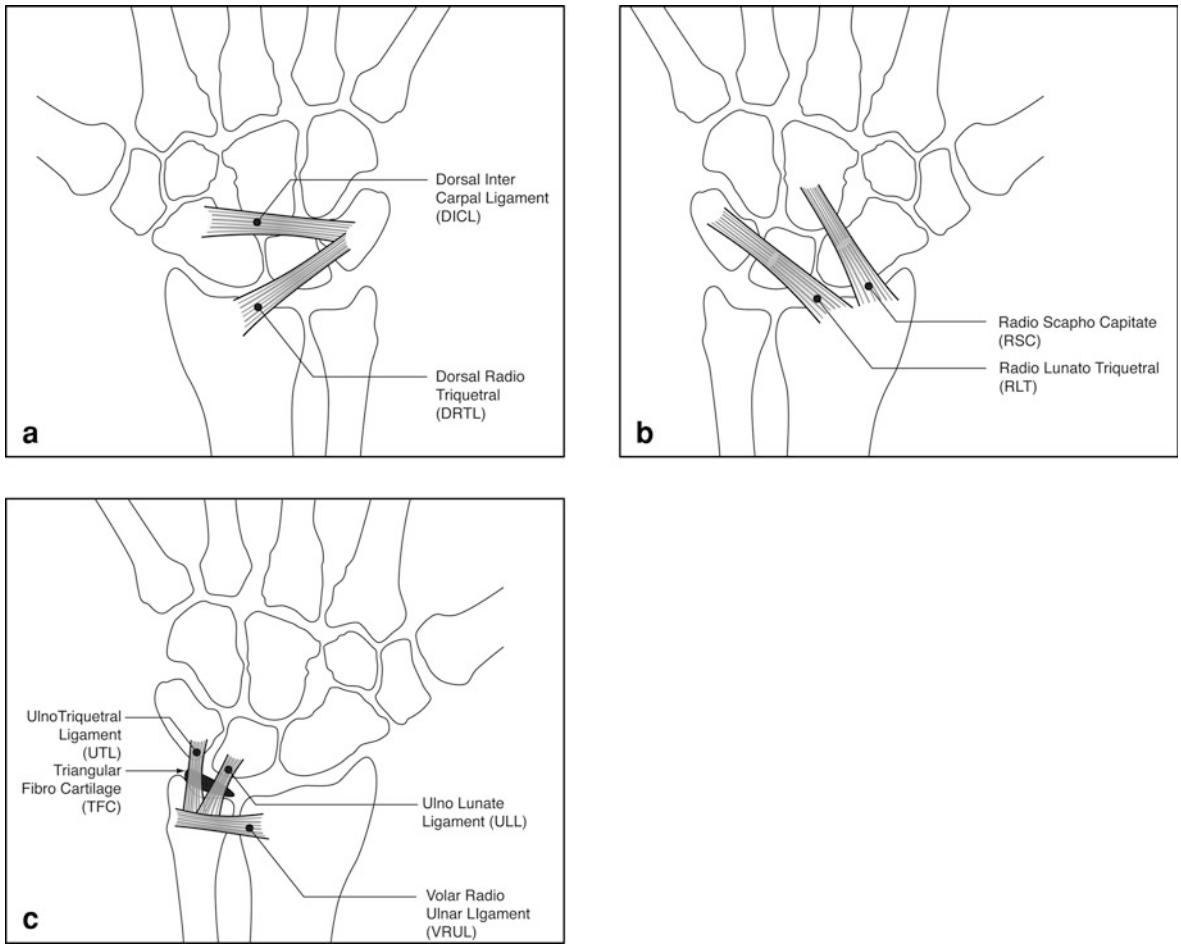

Fig. 3 **a** Important dorsal ligaments. **b** Volar ligaments radial aspect. **c** Volar ligaments and TFC

from the base of ulna styloid to the lunate and triquetral bone. These four ligaments account for the fractures of the ulna styloid seen in several injuries including Colles fractures and distal radio ulna joint disruption (Fig. 3c).

Of the very many intrinsic ligaments, only those connecting scaphoid, lunate and triquetral bones are of significance with respect to acute bony injuries. Thus, the scapho-lunate ligament is disrupted with scaphoid rotatory subluxation.

2 Injuries of Radius and Ulna

Most commonly injuries result from fall on the outstretched wrist. The type of injury sustained is age related.

2.1 Children

In young children, fractures of the radius proximal to the epipyhseal plate predominate in age group 6–10. These fractures often involve both radius and ulna and may be grossly displaced (Fig. 4). After this, until epipyhseal fusion injuries most commonly involve the epipyhseal plate and are thus Salter Harris fractures. Typically, there is dorsal displacement of the epiphysis with or without an associated fracture fragment from the adjacent metaphysis resulting in either a Salter-Harris type one or two injury (Fig. 5). The degree of displacement is often gross, but on occasion the anteroposterior radiograph can appear quite normal. As with adults, it is careful inspection of the lateral film which will reveal the abnormal alignment

Fig. 4 **a** and **b** AP and lateral radiographs demonstrate fracture of radius and ulna in a child. There is considerable angulation and overlap at the fracture site. The fracture is proximal to the epiphysis which is not involved. This is the typical site and appearance of wrist injuries in children under the age of 10

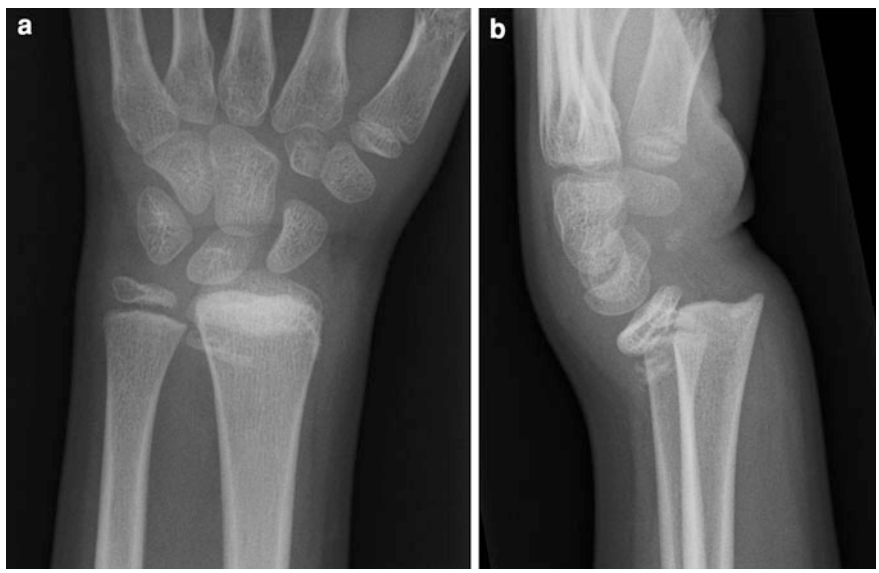

Fig. 5 **a** AP radiograph with no obvious abnormality. Observe however the loss of clarity of the radial epipyhseal plate with increased sclerosis. **b** Lateral radiograph shows that the epiphysis is displaced dorsally. There is a small fragment of bone from the metaphysis in addition which means this is a Salter Harris type 2 injury. This is the commonest type of injury seen at the epipyhseal plate

of the distal radial epiphysis. Colles type fractures do not occur in this age group. Greenstick and buckle or Torus fractures of the radius occur only in children. Torus fractures are a compression failure of bone usually at the junction of diaphysis and metaphysis. The term comes from Latin meaning a "protuberance" or "rounded swelling". The injury is due to compression forces resulting in a circumferential buckling of the cortex. Thus, the abnormality can be seen on both views although it may be more evident on the lateral projection (Fig. 6). It is a relatively minor injury that will heal well with only minimal immobilisation required (Davidson et al. 2001). Scaphoid fractures do not occur in children

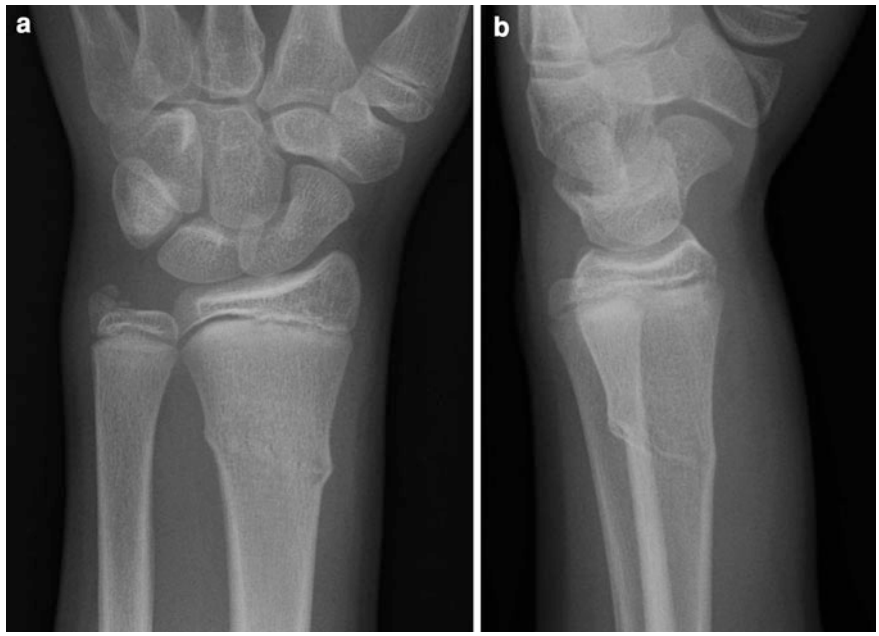

Fig. 6 **a** and **b** There is buckling of the cortex of the radius. This is a circumferential injury and thus seen on both AP and lateral views. It is referred to as a Torus fracture and is seen exclusively in children

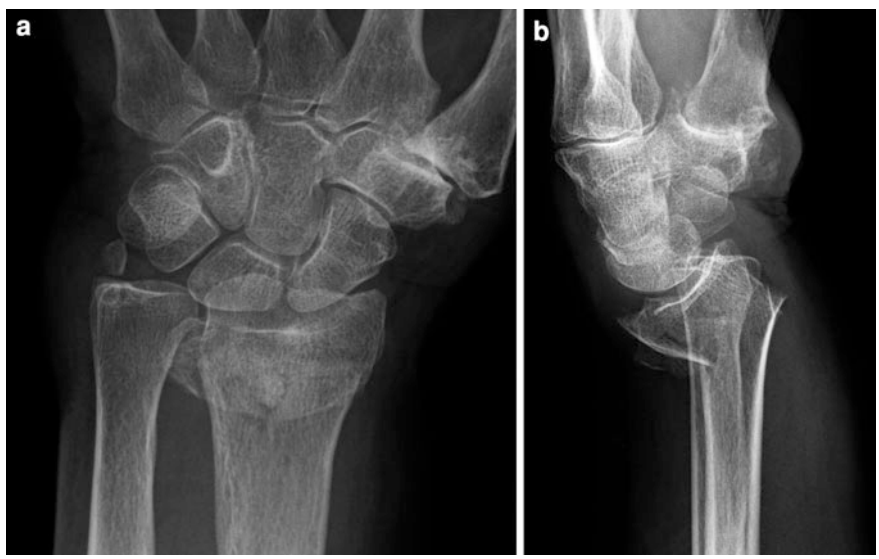

Fig. 7 **a** and **b** Colles fracture. There is fracture of the distal radius with dorsal angulation. The articular surface is not involved. There is some radial displacement, and there is an associated fracture of the ulnar styloid process. All of the above need to be present to fulfil the original description of a Colles fracture

under 10 and are rare in older children (Thornton and Gyll 1999).

2.2 Adults

Colles fracture is the commonest wrist injury in patients over age of 40. Increasing frequency with age suggests a relationship to osteoporosis. It was first defined by Abraham Colles professor of surgery in Dublin in his 1814 paper "On the Fracture of the Carpal Extremity of the radius". His definition includes the following: (1) fracture of radius within 2 cm of distal radial articular surface but not involving it, (2) dorsal angulation of distal fragment, (3) dorsal displacement of the fragment, and (4) associated fracture of ulnar styloid process. In addition, there is also often some lateral (radial) displacement of the distal radial fragment (Fig. 7). The mechanism of injury with resultant forces applied to

Fig. 8 **a** and **b** Smiths fracture. The distal radial fracture fragment is angulated and displaced in a volar direction. The articular surface not involved. There is an associated distal ulna fracture

the distal forearm bones explains these findings. With fall onto the outstretched hand in extension, impact occurs on the thenar eminence. There are compression forces transmitted along the dorsal cortex of the radius with traction forces along the volar aspect. This results in the fracture with displacement described above. The ulnar styloid fracture occurs due to radial shortening with traction on the ulnar styloid process via the triangular fibrocartilage complex principally the ligaments which attach to the process.

Smith (1847) described a variation of the above where the distal radial fragment is displaced and angled volarly and medially. This is typically caused by falling onto the wrist whilst it is flexed. Again a key feature is that the articular surface remains intact (Fig. 8). Subsequently, this fracture has been subclassified by some to include volarly displaced fractures with an intra-articular component. This injury is indistinguishable from the reversed Bartons fracture discussed below.

Barton described an injury of the distal radius (Barton 1838) as follows: "a subluxation of the wrist consequent to a fracture through the articular surface of the carpal extremity of the radius… The fragment… usually is quite small, and is broken from the end of the radius on the dorsal side" (Fig. 9). This fracture differs from Colles and Smiths fractures due to involvement of the articular surface of the radius. It is a shearing injury through the articular surface. The term is now often incorrectly ascribed to any intra-articular fracture. Barton's description also includes the presence of dislocation or subluxation of the radiocarpal joint. A similar injury but with the bone fragment from the volar margin is known by some as a reversed Bartons fracture. It is in fact the volar fracture with volar displacement which occurs more commonly. The fracture fragment varies in size but may involve up to 50% of the articular surface (Fig. 10). The key feature is that the articular surface of the lunate remains in contact with the displaced rim fragment of the distal radius (Fig. 9), and it is this finding that distinguishes this injury from a radio carpal dislocation.

Subtle radial fractures can be easily overlooked. The signs to look for are a subtle crinkle in the cortex of the radius usually on the dorsal aspect and seen only on the lateral film (Fig. 11). Alteration in the radial angle from the usual 10° volar angulation will provide confirmatory evidence but is not present in every case. It has been suggested that soft issue signs around the wrist such as loss of the pronator fat stripe which is normally seen as a lucent area on the volar aspect of the distal radius is a useful adjunct to identifying subtle radial fractures (MacEwan 1964) However, a recent review of the utility of this observation has shown it to be of limited value with a sensitivity of only 26% (Annamalai and Raby 2003).

Isolated fracture of the radial styloid process (Fig. 12) is also known as Hutchinsons or Chauffeurs Fracture. This refers to an intra-articular fracture that

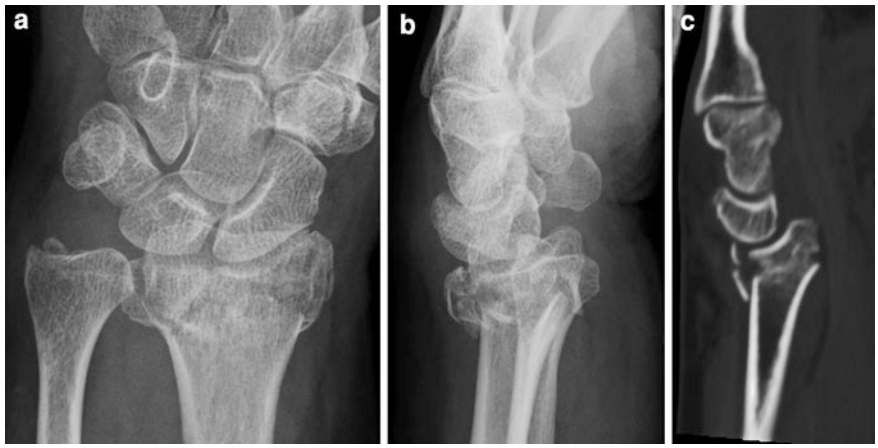

Fig. 9 **a** There is a fracture of the distal radius with extension into the radial articular surface. **b** The distal fracture fragment is angled dorsally, the carpus is subluxed posteriorly. **c** Sagittal CT confirms the intra-articular component of the fracture and the dorsal subluxation of the carpus

Fig. 10 **a** Lateral radiograph with a small fracture fragment of the distal radius on volar aspect. **b** Sagittal CT demonstrates the degree to which the carpus has subluxed volarly. **c** A second case where the volar fracture and carpal displacement is clearly evident on the radiograph. It involves nearly 50% of the articular surface

runs obliquely across the distal radius from the radial cortex into the joint separating the radial styloid from the parent bone. The injury is explained by the ligamentous attachments. The strong RSL and RLT ligaments attach to the radius on the styloid side and result in this avulsion injury.

Die punch injuries occur due to impaction of the lunate on the lunate fossa of the radius which results in a depressed comminuted intra-articular fracture of the radial articular surface which may have both sagittal and coronal components (Fig. 13). The full fracture extent may be difficult to see on plain films, but CT will demonstrate the disrupted articular surface which has both sagittal and coronal components. Depression of the fracture fragments arising in or near the lunate fossa is a key finding. There may be up to four fracture fragments. Commonly, this type of injury is seen as part of a more complex injury of the radius.

The use of eponymous names is prone to misuse. Unless all fully understand precisely what it describes, clinical confusion can result. Many

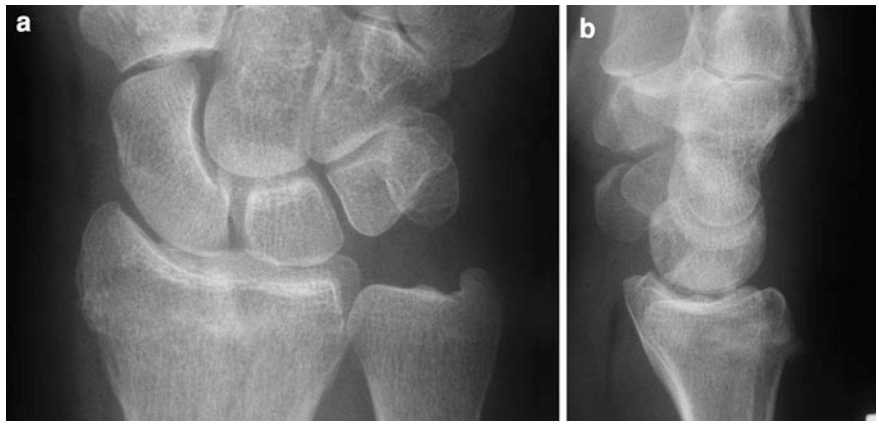

Fig. 11 **a** AP view there is some disruption of the normal trabecular pattern in the distal radius, and there is a slight step of the cortex. **b** On the lateral, there is a subtle buckling of the dorsal cortex. Note that the normal volar tilt of the distal radial articular surface has been reversed

Fig. 12 There is an isolated fracture of the distal radius running obliquely through the distal radius to reach the articular surface. This separates the radial styloid from the rest of the bone

fractures do not fall precisely into any of the exact original descriptions. It must be appreciated that descriptions of injures that now have eponymous names attached were derived from clinical examination and cadaveric studies in the pre radiology era. The variations that can occur with all these injuries were not appreciated at that time. For this reason, it is probably better to give a full description of the fracture lines, fragments displacement and angulation and extent of articular involvement if any. To try and improve on this situation, several classification systems have been proposed (Frykman 1967; Fernández 1993; Melone 1986; Jupiter and Fernandez 1997). These are based variously on the mechanism of injury or the anatomy of the fracture. These systems attempt to provide a framework for treatment options by the orthopaedic surgeon, but none have been universally adopted. Unless locally agreed practice is to use one of the classifications to communicate findings to your orthopaedic surgeons, they are of little practical value to the reporting radiologist on a day-to-day basis. For this reason, they have not been included in this chapter.

2.3 Distal Radio-Ulnar joint

In the acute setting, disruption of the distal radio-ulnar joint (DRUJ) is seen in association with 3 types of fracture.

By far the most common is in association with fracture of the distal radius. Any significant radial shortening may result in disruption of the distal radio ulnar joint. The incidence of this is between 11 and 19% of distal radial fractures (May et al. 2002).

A different circumstance exists with the so-called Galeazzi fracture dislocation. In this event, a fracture of the shaft of the radius occurs with angulation and/or overlap of bone at the fracture site. Unless there is a fracture of the ulna as well, there will be dislocation

Fig. 13 **a** AP radiograph shows abnormality of the distal radius with comminution of the articular surface of the radius on the ulnar side. This is the lunate fossa of the radius. **b** The lateral view demonstrates disruption of the dorsal cortex. The lunate has been driven down onto the radius causing this injury pattern. **c** This 3D volume reconstructed CT is looking from the ulnar side of the wrist (the ulna has been removed). The lunate is seen disrupting the lunate fossa of the radial articular surface

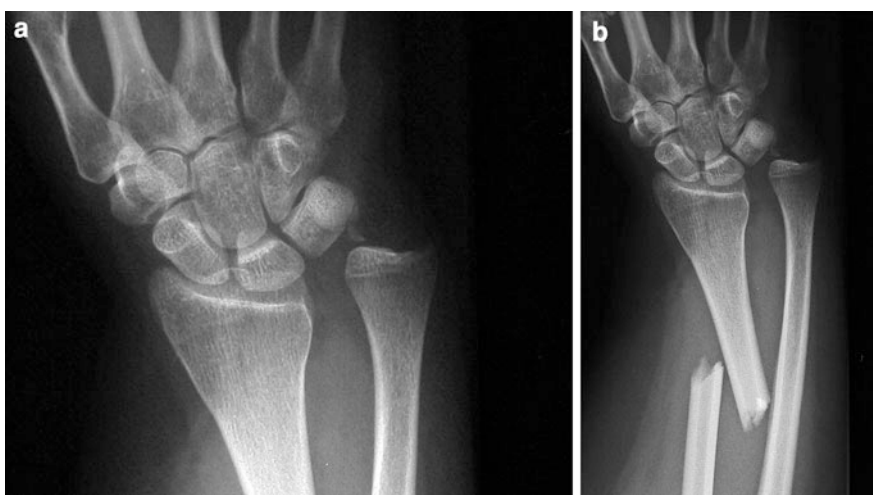

Fig. 14 **a** AP of wrist demonstrates a wide separation and displacement of the distal radio-ulnar joint, It is impossible for this to occur in isolation. There must be a more proximal fracture of the radius with angulation or overlap at the fracture site. **b** Radiograph of forearm demonstrates such a fracture

of the DRUJ. Conversely, if a DRUJ dislocation is evident on a wrist radiograph, then a more proximal radial fracture is likely to have occurred and radiographs of the whole forearm must be obtained (Fig. 14).

The third fracture associated with distal radio ulna joint disruption is the Essex-Lopresti fracture dislocation. This occurs when a fall on the outstretched hand results in an axial force driving the radius proximally with disruption of the DRUJ and the distal interosseous membrane finally resulting in fracture and or dislocation of the radial head. The injury is generally only sustained by a severe force.

Isolated disruption of the DRUJ is much less common and can be difficult to diagnose (Nicolaidis et al. 2000; Tsai and Paksima 2009). It is thought to

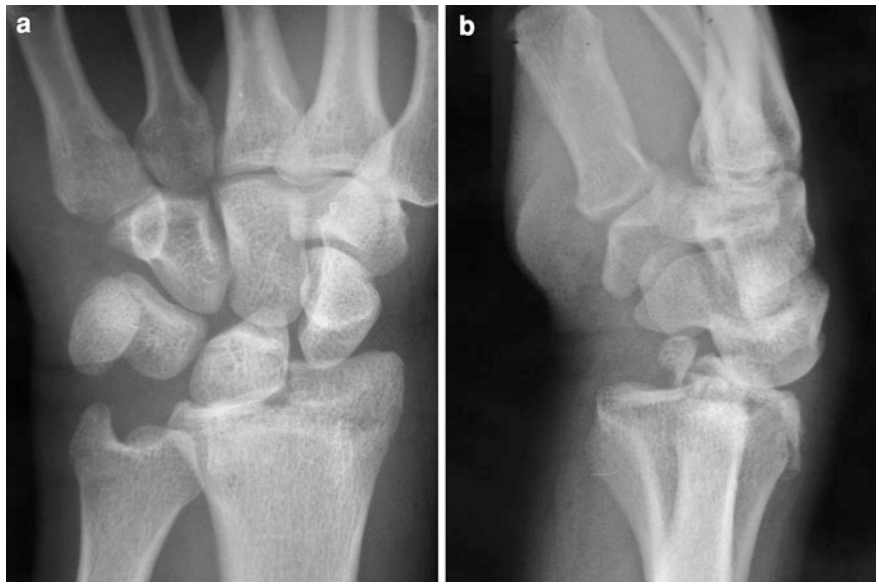

Fig. 15 **a** AP view of wrist with evidence of disruption of the carpal arcs. **b** On the lateral view, the whole carpus is displaced dorsally. The bony fragments on the volar aspect are due to avulsion by the volar ligaments attached to the volar aspect of the radius

occur with hyperpronation with fall on the outstretched hand. A fracture of the ulnar styloid process may be present, but this seen more commonly in association with a radial fracture. DRUJ disruption in turn is associated with injury of the TFCC and the associated stabilising ligaments. Thus, this tends to present more often as chronic wrist pain often with no definite acute incident.

Plain radiographs (Nakamura et al. 1995; Lo et al. 2001) and CT (Nakamura et al. 1996) have been utilised to evaluate the DRUJ, but can be difficult to assess with considerable overlap between normal and abnormal. There is an association between DRUJ disruption, ulna styloid process fracture and damage of the underlying TFCC.

Radiocarpal fracture dislocations (RCFD) are rare and occur due to high-energy injuries with both shearing and rotational components (Ilyas and Chaitanya 2008). They can occur in isolation but more commonly are associated with fracture of the distal radius. Dorsal displacement is more common than volar (Fig. 15). These injuries need to be differentiated from the Bartons fracture where a rim fracture of the radius is also present. In the Bartons fracture, the radial articular surface remains in contact with the proximal carpal row. With RCFD, the radial articular surface is no longer in alignment with the carpal row. This is best appreciated on the lateral radiograph by observing the position of the lunate relative to the radius. The dislocation may occur in isolation, but often a dorsal dislocation is associated with a volar rim fracture of the radius. This apparent paradox is explained by the ligamentous attachments. When the carpus dislocates dorsally, the volar extrinsic ligaments attached to the volar rim of the radius may avulse a bone fragment from this site (Lozano-Calderón et al. 2006). RCFD are also associated with intra-carpal fractures and fracture dislocations (see below).

There are two classifications for these injuries. Moneim et al. (1985) classified these injuries into 2 groups depending on whether there was associated intercarpal injury or not. An alternative classification is based on the size of the radial fracture fragment (Dumontier et al. 2001). In those with no or only a small radial fragment, there is likely to be major ligamentous disruption resulting in multidirectional instability. In those with a large radial styloid fragment separated from the underlying bone, the radiocarpal ligaments are likely to be intact. Reduction of the dislocation with fixation of the fracture is likely then to restore wrist stability.

3 Carpal Injuries

3.1 Scaphoid

The scaphoid is by far the most common of the carpal bones to sustain an injury and accounts for at least

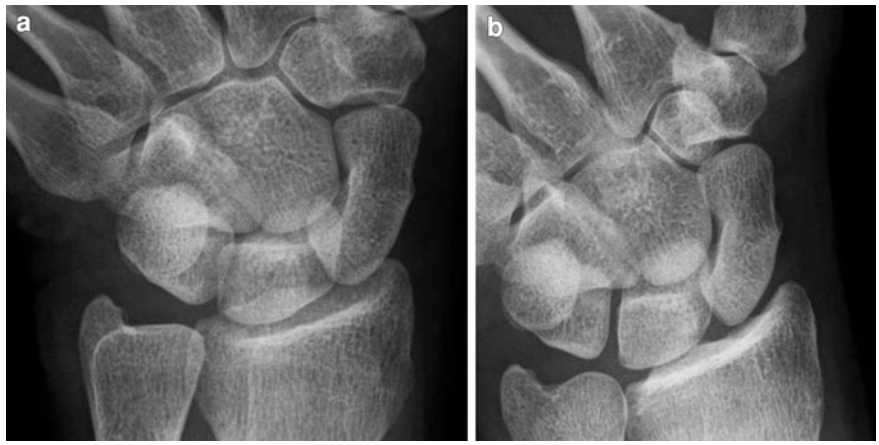

Fig. 16 In addition to the conventional AP and lateral views of wrist, if a scaphoid fracture is suspected, then additional view must be obtained. These are with **a** ulnar deviation of the wrist and **b** deviation and angulation of the tube towards the elbow

Table 1 Relative incidence of carpal bone fractures

Scaphoid	68.2%
Triquetrum	18.3%
Trapezium	4.3%
Lunate	3.9%
Capitate	1.9%
Hamate	1.7%
Pisiform	1.3%
Trapezoid	0.4%

60% of all carpal fractures (Gaebler 2006; Table 1). The propensity for this bone to fracture more often than all the other carpal bones combined is explained by its anatomy. Unique among the carpal bones the scaphoid bridges the proximal and distal carpal rows. As these two rows move to different degrees during wrist dorsiflexion, this places increased stress on the bridging scaphoid. This is compounded by the presence of the radiocapitate ligament that lies across the waist of the scaphoid. Both of these forces act to maximise the stress forces at the waist of the scaphoid thus accounting for the high incidence of injuries at this site. Furthermore, in extreme dorsiflexion, the scaphoid waist may impact upon the dorsal rim of the radius providing an additional mechanism of injury.

Radiography The scaphoid lies at about the angle of about 45° relative to the radial shaft in the sagittal plane. It is overlapped by the lunate, capitate and pisiform on the lateral view. Hence, the two conventional views of the wrist may fail to demonstrate some scaphoid fractures. With the PA view in particular, the X-ray beam passes obliquely through the scaphoid rather than at right angles to it, so a fracture line through the waist of the scaphoid will be traversed obliquely by the beam. Therefore, unless the fracture is widely separated, it is often not detected on this view. To overcome these problems, it is essential when a scaphoid injury is suspected clinically that additional dedicated views are obtained. Typically, 2 more radiographic projections are employed with the intention of elongating the scaphoid, projecting it clear of other carpal bones and allowing the X-ray beam to pass through the scaphoid perpendicular to its long axis. The projections used vary, but in the authors department a second PA view with ulnar deviation plus one with the tube angled at 45̊ towards the elbow is obtained (Figs. 16, 17).

This small bone causes more diagnostic and management difficulties than almost any other due to the nature of its blood supply. Its blood supply is unusual with the blood entering the distal pole first then passing into the proximal pole. The result is that when fracture occurs through the waist of the scaphoid which is the commonest site (80% of cases) and the proximal pole (10%) the blood supply to the proximal pole is interrupted (Fig. 18). This brings with it the danger that the proximal pole loses its vascular supply and develops avascular necrosis. Fractures of the waist are associated with 30% incidence of AVN, and disruption of the proximal pole almost always leads to this complication (Fig. 19). Alternatively, the lack of blood supply hinders healing at the fracture site and non-union of the fracture occurs (Fig. 20).

Fig. 17 Effect of scaphoid views. **a** Conventional AP view does not show any definite abnormality. **b** Angled view clearly demonstrates a now obvious fracture

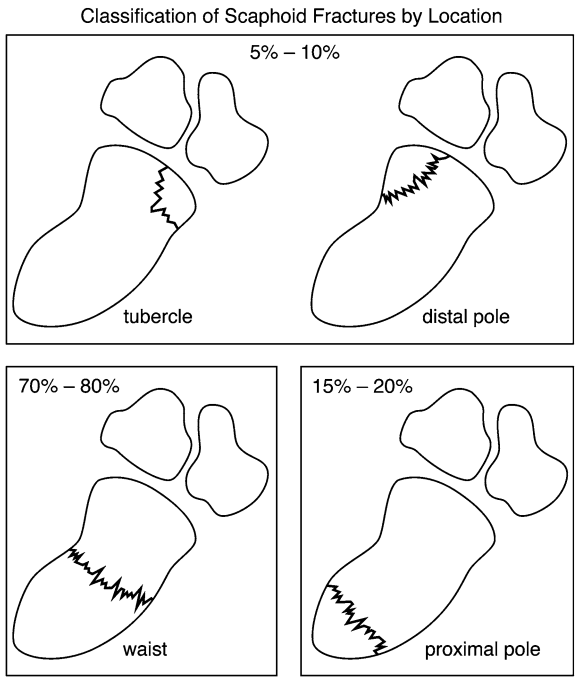

Fig. 18 The sites of scaphoid fracture with frequency of occurrence. Fractures of the waist account for the great majority

Fig. 19 Initial radiograph taken at time of injury demonstrated a fracture of the waist of the scaphoid. This radiograph taken 18 months later shows that the fracture line remains well demarcated with sclerotic edges. This represents established non-union of the fracture

Historically, extreme care has been taken in managing patients with suspected scaphoid injuries. Because of the difficulties that may occur in identifying scaphoid fractures on radiographs, a combined clinical and radiological approach has been adopted to minimise the possibility that a fracture has been over looked. In patients with an appropriate history and clinical findings suggestive of scaphoid fracture, an initial scaphoid series of radiographs is obtained. If a fracture is identified, the wrist is immobilised and managed accordingly. If no fracture identified, it is recognised that this does not completely exclude a fracture due to the difficulties described above. Accordingly, because of the possible long-term complications that may arise after suboptimal treatment of a fracture the patient is managed as if a fracture is present and the wrist is immobilised. The patient is then reviewed at about 10 days when further radiographs are obtained. It is stated that resorption

Fig. 20 The proximal pole of the scaphoid is sclerotic and shrunken. This is the appearance of established avascular necrosis some 5 years after initial injury

Fig. 21 Multislice CT with coronal reconstruction demonstrates a fracture of the scaphoid. No abnormality was evident on the plain radiographs

will occur around a fracture site rendering it visible on delayed radiographs. This process may need to be repeated on several occasions until either a fracture is clearly identified or the patient's symptoms resolve. "We overtreat a lot of patient to avoid undertreating a few" (Barton 1992).

This practice or similar modifications remain in common use (Brookes-Fazakerley et al. 2009); however, it has been questioned in the era of more sophisticated imaging options. To understand the validity of the management rationale, some basic back ground information is required.

How many fractures are present but not visible at the time of the initial radiographs?

Most studies have shown that in fact a great majority of fractures (85% or more) are visible on the initial films (Leslie and Dickson 1981; Brøndum et al. 1992). Some even consider that all fractures can be identified (Duncan and Thurston 1985).

How many patients develop non-union or avascular necrosis?

The same authors independently found that these complications occurred in 5% of patients with a scaphoid fracture.

How often are fractures identified on follow-up films?

In a recent study using MR as the gold standard, it was found that detection of occult fractures on follow-up films was extremely inaccurate, with sensitivity as low as 9% and very poor interobserver reliability (Low and Raby 2005). This confirmed observations by others (Tiel-Van Buul et al. 1992a, b). It is apparent that clinicians rely on clinical findings rather than radiographs to guide management.

To improve on this situation, for many years other imaging modalities have been utilised including isotope bone scan CT and MRI. A recent international survey (Groves et al. 2006) however has shown that despite the extensive evidence base the majority of departments still undertake repeat radiographs when no fracture is seen. Alternative imaging modalities are employed only as a secondary investigation and in order of frequency these are MR CT and isotope scan.

Isotope bone scans are sensitive but non-specific. Whilst almost all fractures will show evidence of increased isotope uptake if scanned 3 or more days after the acute event, approximately 35% of increased isotope up take in the carpus is due to abnormality other than a scaphoid fracture, and additional imaging may be needed to resolve this issue (Tiel-Van Buul et al. 1992a, b; Tiel-Van Buul et al. 1993; Waizenegger et al. 1994; Beeres et al. 2007).

CT is utilised more than isotope scans (Groves et al. 2006). Whilst CT can undoubtedly identify some occult fractures (Fig. 21), there is still an error rate (Adey et al. 2007), and it has been shown that trabecular bone injury will not be detected although the relevance of this is debatable (Memarsadeghi et al. 2006; La Hei et al. 2007).

MRI Is now the investigation of choice (Foex et al. 2005), but use remains limited due to perceptions that

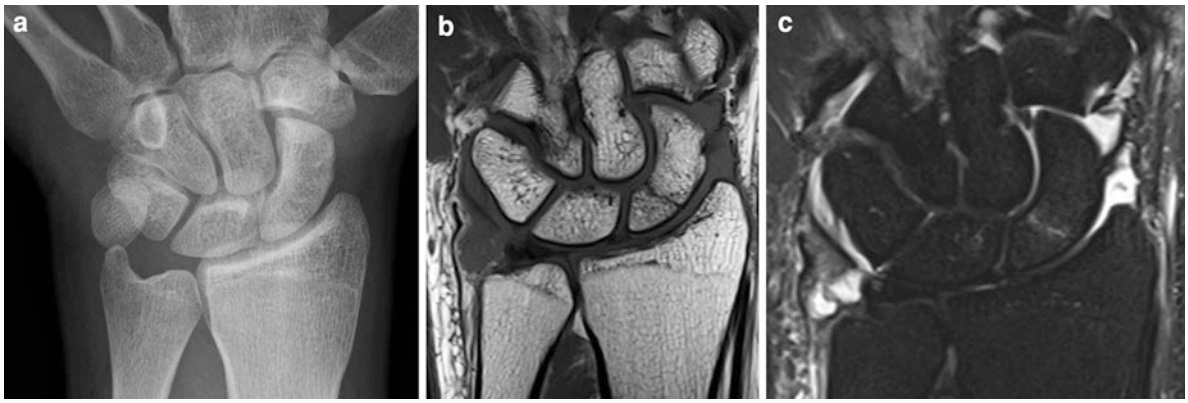

Fig. 22 **a** Radiographs are normal. No scaphoid fracture identified on any view. **b** and **c** Coronal T1-weighted and STIR MR demonstrates a fracture across the scaphoid waist seen as a low signal linear line on the T1-weighted and high signal line on the STIR sequence

its availability is restricted. There is extensive literature regarding the use of MR in patients with suspected scaphoid fracture not evident on plain film (Fig. 22) (Raby 2001; Brydie and Raby 2003). This consistently indicates that MR accurately identifies scaphoid fractures, and other carpal or radial fractures that may be responsible for the patient's symptoms. Just as importantly a normal MR will exclude bony injury allowing early discharge of the patient from hospital care, and it is this fact that renders it cost effective (Kumar et al. 2005). Several studies have confirmed this to be the case. The ability to be able to reliably discharge patients without need for immobilisation, further hospital attendance or repeat radiographs is the most important benefit of this strategy (Dorsay et al. 2001).

Despite the best efforts of all concerned in the management of patients with scaphoid fractures, non-union or AVN still occurs in a small proportion of patients. Attention has thus been directed to imaging techniques that may indicate that a recognised fracture is either failing to unite or developing AVN in the hope that early detection of these complications would allow early intervention (Figs 23, 24). To date, evidence of ability to reliably detect these complications is limited. The major focus has been on the use of MRI with contrast enhancement. The theory is that as fracture of the scaphoid waist may interrupt the blood supply to the proximal pole, then on contrast enhanced scans lack of enhancement of the proximal pole will indicate lack of blood supply and thus poor prognosis with non-union or avascular necrosis as a long-term result (Dawson et al. 2001). Studies have had conflicting results, and the numbers in the studies have been small (Singh et al. 2004; Cerezal et al. 2000) There is no good evidence that contrast-enhanced MR can accurately predict either of these complications. However, whether or not these complications are detectable earlier by imaging is of little consequence if the final outcome remains unaltered. To date, there is no robust evidence that there is any improvement in outcome as a result of contrast-enhanced MR, and one study has shown no outcome benefit in a group of patients who underwent MR prior to surgery (Singh et al. 2004). Further studies with accumulation of large data sets are required to confirm or refute its value.

CT also has its advocates (Smith et al. 2009) with a recent paper suggesting benefit in the detection of AVN and non-union with improved outcome after surgery. Confirmatory evidence from other sources is awaited. CT however is undoubtedly of value in detecting certain other complications of scaphoid fracture. Some scaphoid fractures unite satisfactorily but may develop the so-called hump back deformity (Fig. 25). This occurs when the distal fracture fragment flexes in a palmer direction with the distal carpal row whilst the proximal fragment rotates dorsally with the proximal carpal row. This results in angulation occurring at the fracture site with a prominent dorsal bony protrusion and is best appreciated on CT. It is associated with persisting pain, restriction of movement and development of arthritic changes. CT can also assist in confirming that a fracture has united

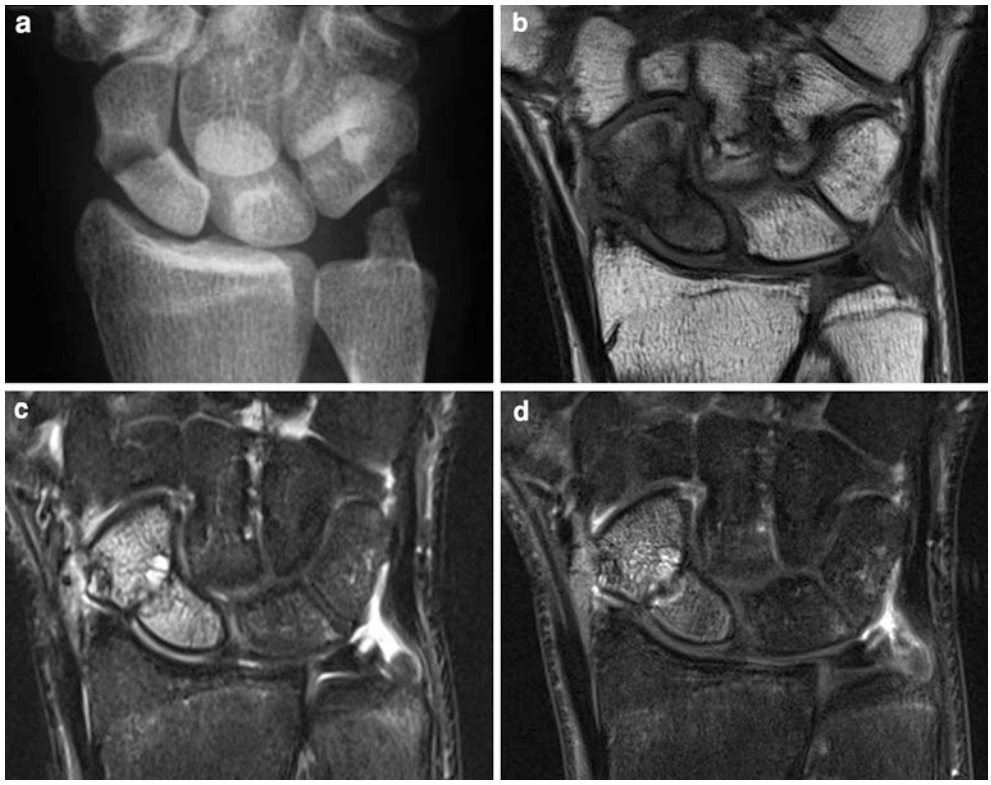

Fig. 23 **a** Radiograph shows scaphoid waist fracture with cystic bone resorption 5 months after initial injury. **b** Coronal T1-weighted image. There is loss of normal marrow signal in the proximal pole. **c** STIR sequence shows diffuse high signal indicating marrow oedema. **d** Post-contrast T1 weighting with fat saturation shows enhancement of the proximal pole suggesting it retains a vascular supply

when plain films suggest that a fracture line persists (Fig. 26).

3.2 Other Carpal Fractures

After the scaphoid, the triquetral bone is most commonly injured accounting for 18–20% of injuries (Table 1). This injury is usually due to a bony avulsion of the insertion of the radio and ulno triquetral ligaments. Typically, the fracture is not evident on the PA view but can be seen on the lateral as a bone fragment seen on the dorsal aspect of the wrist (Fig. 27). Transverse fracture can also occur due to extreme dorsiflexion with compression of the triquetrum between the ulna and hamate. These fractures may be seen in association with Perilunate dislocation (see below).

Other carpal bone injuries are all relatively rare, each of the other carpal bone accounting each for only 2–3% of injuries. CT or MR may have a useful role to play in these injuries that are often difficult to detect on plain films.

Fractures of the hamate can involve the hook in isolation or the body. Hook fractures are often associated with sporting activities since the handle of a bat or racquet abuts the hook. Conventional radiographs will often fail to demonstrate such injuries that may therefore be diagnosed as soft tissue injuries or "wrist sprain" only (De Schrijver and De Smet 2001). Additional views have been shown to demonstrate these fractures such as the so-called carpal tunnel view. However, if such a fracture is strongly suspected clinically, then CT will demonstrate them most clearly (Fig. 28) (Kato et al. 2000). Fracture of the body can occur in isolation but more often are associated with other carpal fractures or with fracture dislocation of the 5th metacarpal base. These injuries are usually evident on conventional radiographs (Fig. 29).

Capitate fractures in isolation are uncommon. Typically, fractures occur through the waist of the

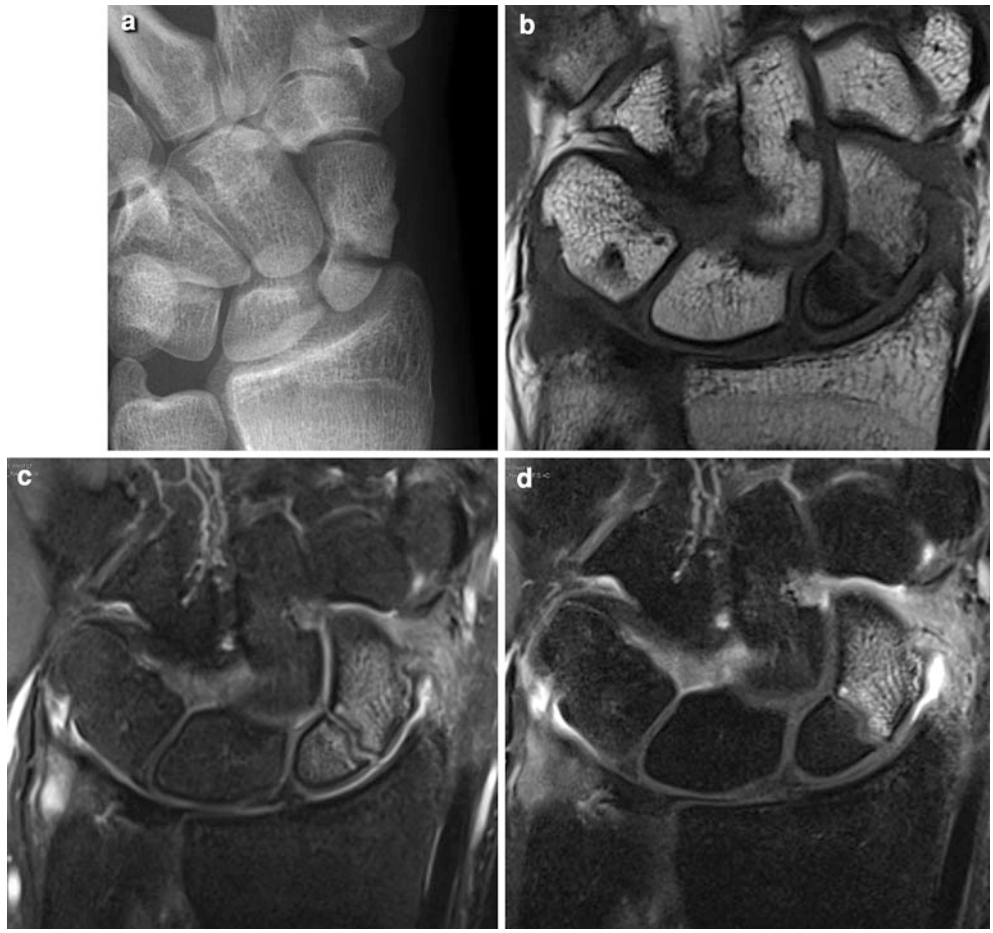

Fig. 24 **a** Fracture of scaphoid proximal pole now 6 months old. **b** There is complete loss of normal marrow signal in the proximal pole on T1-weighted image. **c** PD fat-saturated image shows diffuse marrow oedema. **d** Post-contrast T1-weighed with fat saturation. There is no enhancement of proximal pole suggesting loss of blood supply

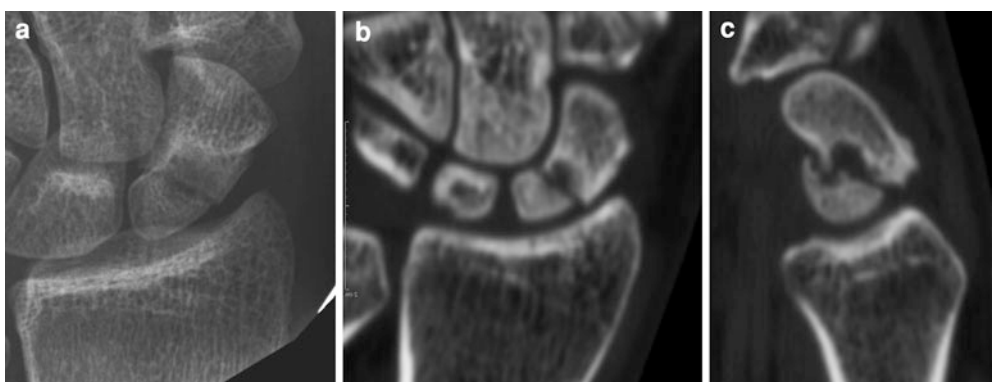

Fig. 25 **a** Radiograph shows a fracture across the proximal third of the scaphoid. Resorption at fracture site has resulted in cystic change at the fracture line. **b** CT undertaken to confirm non-union. There is no evidence of any bony continuity at the fracture site. **c** Sagittal reconstruction demonstrates displacement at the fracture site resulting in the so-called hump back deformity

Fig. 26 **a** Radiograph of scaphoid fracture after 6 months. The fracture line persists suggesting possible non-union. **b** Coronal reformatted CT. The scaphoid is sclerotic with a linear lucency across the waist suggesting non-union. **c** Sagittal reformatted CT shows that in fact there is bony union across the majority of the fracture site. A step in the cortex is the cause of the linear lucency seen on the previous images mimicking a persistent fracture line

capitate. These can be seen on the AP view of the wrist (Fig. 30). More commonly capitate fractures occur in association with perilunate dislocation. Fractures occur as a result of wrist dorsiflexion. With more severe injury, the proximal pole of the capitate can be displaced and rotated through either 90° or 180° (Fig. 31). These findings are seen along with other fractures of the greater arc or zone of vulnerability.

Lunate fractures are uncommon and typically are small chip or avulsion fractures. Only occasionally do the fractures extend through the bone. The principal complication is that of avascular necrosis (Keinbock's disease). Pisiform and trapezoid fractures are rare and are not considered further.

3.3 Carpal Dislocations

The proximal carpal row (scaphoid, lunate and triquetral) act as a functional unit and is referred to as an intercalated (inserted in between) segment. That is a functional row of bone inserted between the distal radius and the distal carpal row. These three bones act as a keystone coordinating wrist motion and transmitting force between wrist and hand. The proximal row of carpal bone has no tendons attached and relies on complex ligamentous attachments as well as bony configuration for stability. The pisiform although it lies proximally is not functionally associated with these bones. It is a sesamoid bone within the tendon of flexor carpi ulnaris.

The distal row of trapezium, trapezoid, capitate and hamate is more stable and forms a transverse arch supporting the metacarpal bones. The distal row of carpal bones are rarely disrupted unless associated with other injuries (see below). The scaphoid that lies at an angle bridges the proximal and distal carpal row and normally contributes to stability of the carpus. Fractures of the waist of the scaphoid break this bony linkage between the two rows. Most carpal fractures and dislocations occur due to falling on the

Fig. 27 This lateral radiograph shows several bone fragments on the dorsal aspect at mid-carpal level. This finding almost invariably indicates a triquetral fracture although the AP view will usually be normal. Further investigation by cross-sectional imaging to prove the origin of the bone fragments is generally not required or indicated

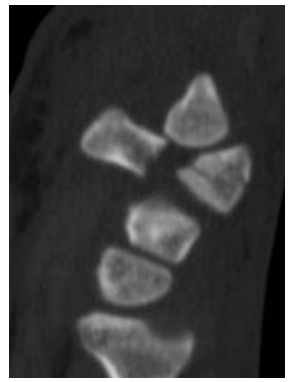

Fig. 28 Sagittal CT demonstrating a fracture of the hook of the hamate. This was not visible on conventional radiographs

outstretched wrist with the wrist forced into a hyperextended position. Evaluation of these injuries is aided by the evaluation of lines or arcs drawn through the carpus. Somewhat confusingly this nomenclature does not relate to the same arcs used to describe normal carpal alignment (Yeager and Dalinka 1985). In this terminology, the lesser arc separates the lunate from the adjacent carpal bones (Fig. 32). The greater arc passes through the scaphoid, capitate, hamate, triquetral (and in some modifications the distal radius and ulna). Injury through the lesser arc represents a lunate dislocation. Injuries of the greater arc indicate a perilunate injury. This may be an isolated perilunate dislocation or with associated fracture(s) of bones along this arc. Virtually, all combinations of fracture can occur along this zone. This is best referred to as the "Zone of Vulnerability" (Johnson 1980). An abnormality anywhere along this arc should prompt a thorough search of all points to identify associated fractures. Injuries of the greater arc are twice as common as those of the lesser arc.

Carpal dislocations thus most commonly involve the proximal row of bones, and the lunate is most often involved. Understanding the lateral radiograph

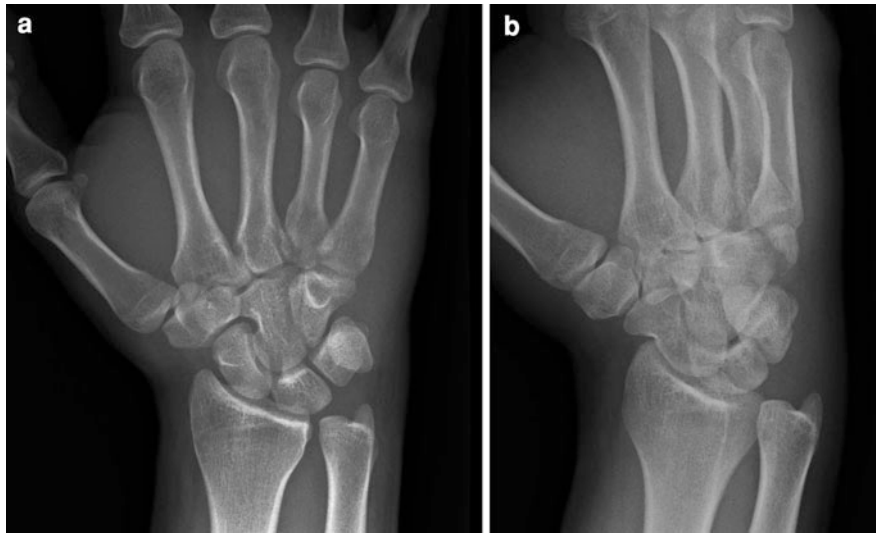

Fig. 29 **a** AP radiograph of wrist is normal. **b** Oblique view demonstrates a vertical fracture of the hamate

Fig. 30 There is fracture through the proximal third of the capitate. This is unusual in isolation

is key to detect these injuries although valuable information is also available on the PA view. On a normal lateral view of the wrist, there should be alignment of the lunate with the distal radius and the capitate. That is to say that a line drawn through the centre of the lunate should inferiorly pass through the radial articular surface and superiorly should pass through the centre of the capitate (Fig. 33). If this rule is broken, a carpal dislocation is certain. We (Raby et al. 2005) have likened this to a saucer (the radial articular surface) with a cup (the lunate) sitting on it. Within the cup, there should sit an apple (the capitate). Lunate dislocation occurs with hyperextension injuries. On a PA radiograph, the normal intercarpal

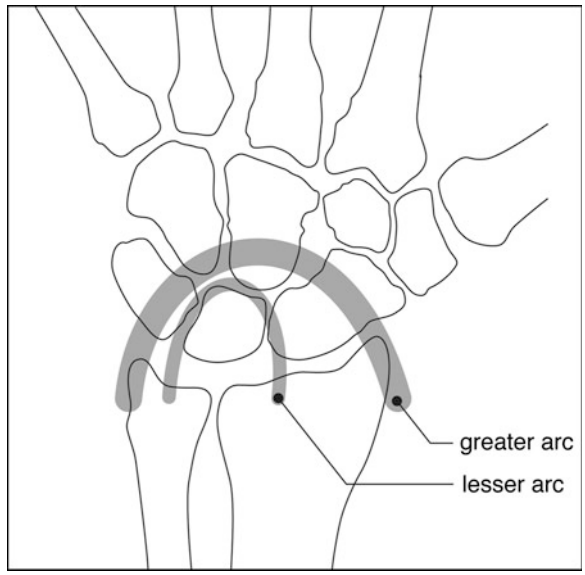

Fig. 32 Carpal fracture dislocations occur along the greater arc or zone of vulnerability

distances are disrupted with bony overlap evident. The lunate appears to have a triangular shape where normally it has a trapezoid appearance. It is on the lateral film however where the diagnosis is most easily detected. Here, a dislocated lunate will be seen displaced to the volar aspect. It is rotated so that is has the appearance of a new moon (Fig. 34). The alignment of the radius and capitate is preserved, but the lunate (the cup) lies palmer to the line drawn through the radius and capitate. Lunate dislocation is most

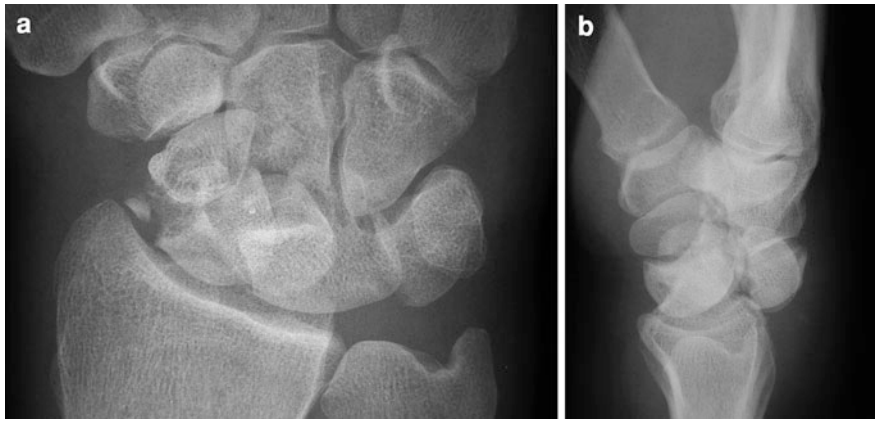

Fig. 31 **a** Complex mid carpal fracture dislocation. There are fractures of the scaphoid and proximal third of the capitate. **b** On the lateral view, the proximal capitate articular surface can be seen rotated through 90° lying dorsal to the lunate. There is perilunate dislocation of the carpus. Capitate fracture are more commonly seen in association with these mid-carpal injuries

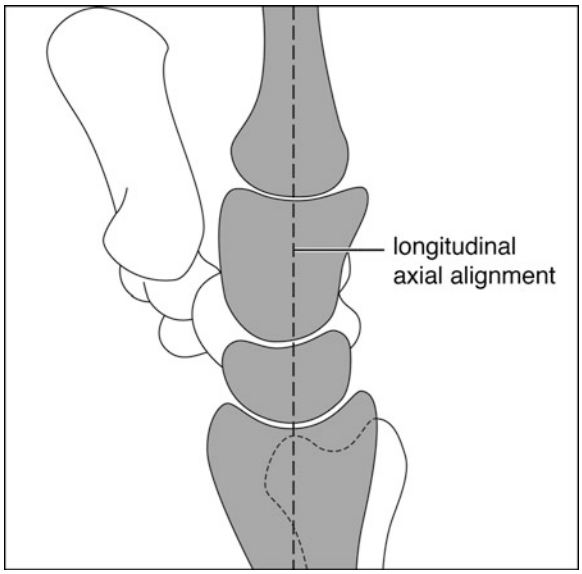

Fig. 33 The normal alignment of the three key bones on the lateral view. The capitate sits on the lunate which sits on the radius. A line drawn through the capitate should pass through the approximate centre of the lunate and distal radial articular surface

commonly an isolated finding with additional fractures found only uncommonly. The maxim "the cup should never be empty" is a simplistic but effective way of detecting these injuries.

Perilunate dislocation is also a hyperextension injury and is often associated with other carpal injuries (see above) most commonly a fracture of the scaphoid. It is more common than lunate dislocation. In this injury, the lunate remains aligned with the radius, but the capitate and the rest of the distal carpal row are displaced in a volar direction (Fig. 35). For this to occur, there must be disruption of some of the intra-carpal ligaments. The injury is often not apparent on the PA views, but on the lateral film the lunate (cup) remains on the saucer (distal radius). The capitate (apple) does not sit in the cup but lies posterior (volarly). As already seen perilunate dislocation is typically associated with other fractures along the greater arc zone of vulnerability (Fig. 36). When there are both fractures and perilunate dislocation present, the convention is to describe first the fractures then the dislocation. In this case, the description should be of a trans-scaphoid, trans–triquetral and perilunate dislocation.

Scapho-lunate disassociation is also known as rotatory subluxation of the scaphoid. It is a ligamentous injury occurring with forced wrist extension. Several ligaments are disrupted in this injury. In sequence, the radioscaphoid, the volar radiocapitate and finally the scapho-lunate ligament fail. This allows the distal scaphoid pole to rotate in a volar direction. On plain radiographs, the injury can be identified by noting a widening of the intercarpal distance between scaphoid and lunate. This is the so-called Terry Thomas sign. The rotation of the

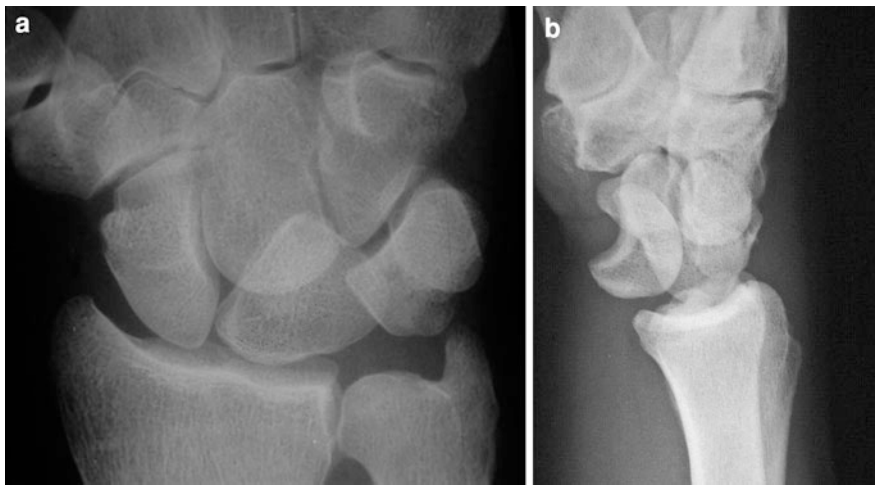

Fig. 34 **a** There is disruption of the proximal carpal arc with interruptions at the junctions of lunate with the scaphoid and triquetral. The lunate has a triangular configuration compared with the normal quadrilateral shape. **b** Lateral view demonstrates loss of the normal alignment of the radius, lunate and capitate with the lunate rotated and displaced volarly. These are all signs of lunate dislocation

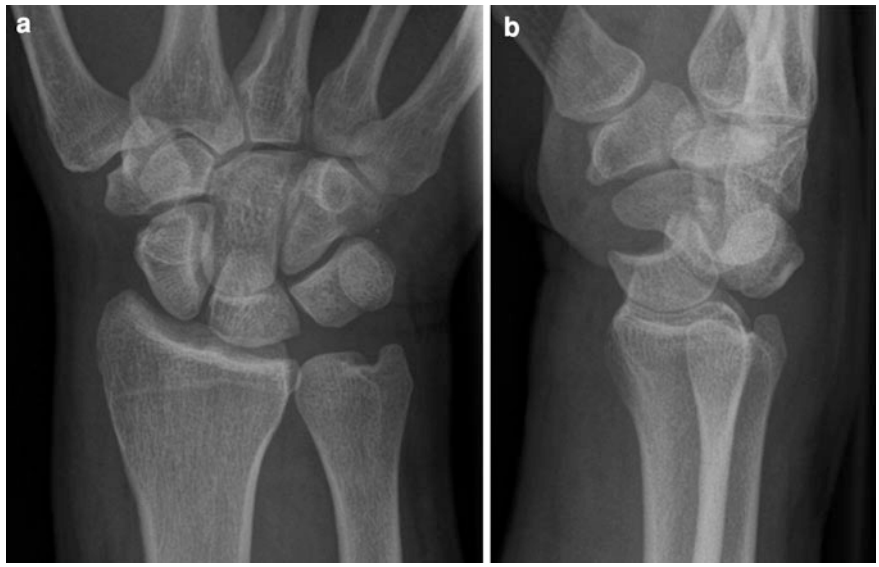

Fig. 35 **a** There is little to see on the AP view of the wrist apart from the triangular configuration of the lunate. The arcs are maintained. **b** On the lateral view, however, there is loss of the normal carpal alignment. The lunate sits normally on the radius, but the capitate now lies dorsal to the lunate indicating a perilunate dislocation. The cup of the lunate is empty

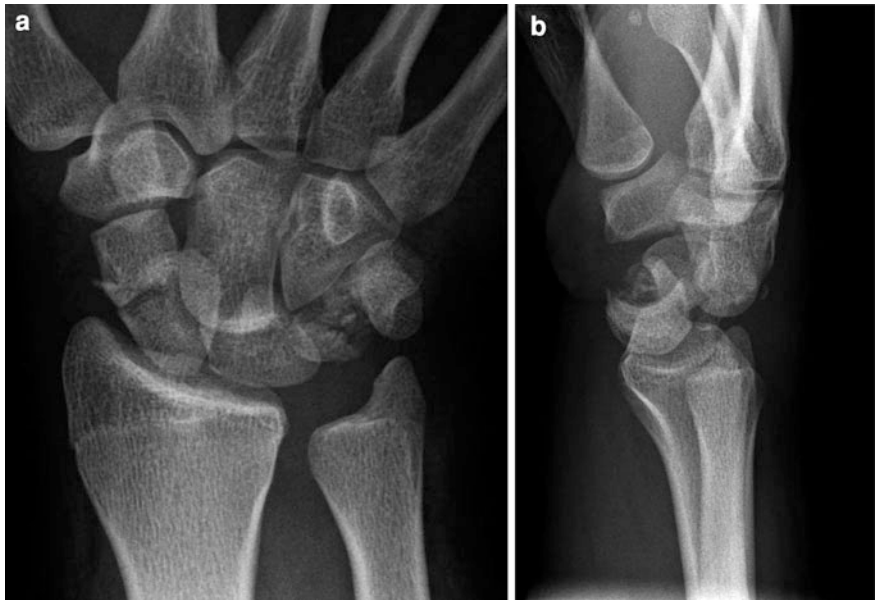

Fig. 36 **a** AP radiograph demonstrates fractures of the waist of the scaphoid and triquetral bones. There is disruption of the second carpal arc with loss of the normal intercarpal spacing. There is marked overlap of both scaphoid and lunate with the capitate. The lunate has an abnormal triangular appearance. **b** The lateral view demonstrates the capitate does not sit on the lunate but lies dorsal to it. This is a trans-scaphoid trans-triquetral perilunate dislocation

scaphoid causes it to be foreshortened, and the distal pole seen end on has a ring-like appearance (Fig. 37) (Hudson et al. 1976). On occasion, the radioscaphoid ligament avulses a bone fragment from the radial styloid attachment, but more often there is no fracture evident so that this is injury that can be easily overlooked.

4 Carpo-Metacarpal Injuries

There is normally little movement at the carpo-metacarpal joints. Strong ligaments bind the distal carpal row to the base of the metacarpals, and there is little movement possible either on palmer or

Fig. 37 There is widening of the gap between lunate and scaphoid. The scaphoid has rotated and appears foreshortened. There is a ring-like appearance of the distal pole due to the pole now being seen end on. This indicates disruption of the scapholunate ligament. Known correctly as rotatory subluxation of the scaphoid, it has been known as the "Terry Thomas sign" in the UK after an actor who had a large gap between his front teeth

Fig. 38 AP radiograph of wrist. There is loss of the carpometacarpal spaces with increased bone density at the base of the 2nd and 3rd metacarpals due to bone overlap indicating dislocation at this site

dorsiflexion. Dislocations at this site only rarely occur in isolation and are more commonly associated with fractures of the metacarpal bases or the adjacent carpal bones, most commonly the hamate and capitate. These injuries are rare and result from high-energy axial loading of the metacarpals such as occurs when delivering a punch. The site of injury often leads to request from the referring clinician for radiographs of the hand rather than the wrist. An AP and oblique view will be obtained.

Disruption of the carpo-metacarpal joint may occur in isolation or may be associated with fracture of either the proximal metacarpal or the adjacent carpal bone. Isolated dislocations without associated fracture are difficult to identify. These injuries can be detected by observation of the loss of the normal gaps between the distal carpal row and the base of the metacarpals and/or by identifying areas of increased bone density due to the resultant bone overlap (Fig. 38). Fisher et al. (1983) described the appearance of the carpometacarpal joint from the second to fifth metacarpal as having an elongated M shape. The articular surfaces of the metacarpals and adjacent carpal bones form two parallel lines with this M shape. Loss of this normal configuration should alert the viewer to a possible metacarpal dislocation. All of these findings are best seen on the AP view. Where there is suspicion on the standard radiograph series, a lateral of the hand may add further useful information. The displaced metacarpal will then be visible as almost all are dislocated dorsally (Fig. 39). Metacarpal fractures when present aid identification of the injury. Carpal fractures may be impossible to see on plain films and may only be evident on subsequent CT (Fig. 40) (Kaewlai et al. 2008; You et al. 2007). A common injury is that of fracture dislocation of the 5th metacarpal, and this accounts for 50% of single ray dislocations. It is likely that this is due to the attachment of the extensor and flexor carpi ulnaris tendons to the 5th metacarpal base which draw the dislocated bone proximally resulting in bony overlap. The second metacarpal accounts for 25% of solitary dislocations. Multiple dislocations are more common. Dislocation of the 5th metacarpal plus one or more of the other metacarpals accounts for 80% of injuries at this level (Rodgers 2001).

5 Acute Soft Tissue Injuries

In acute trauma, soft tissue injuries are common but are usually overshadowed by the presence of bony fractures and dislocations. Thus, injuries of the

Fig. 39 **a** AP and oblique radiographs of wrist and hand. There is loss of the normal carpal-metacarpal spacing at the base of the 3rd to 5th metacarpals. Increased sclerosis is also evident, meaning there must either be bone impaction or overlap. **b** An additional lateral view demonstrates dorsal dislocation of the metacarpals

Fig. 40 **a** Loss of carpo-metacarpal space at 5th metacarpal. Note also there is loss of alignment of the third metacarpal with the capitate. **b** Sagittal CT image demonstrates dorsal dislocation of a metacarpal with fractures of the capitate. **c** Axial CT image shows fractures of capitate and hamate. CT will often identify additional fractures in this type of injury

Table 2 Palmer classification of TFCC tear

Traumatic injury	Comments
A. Central perforation	
B. Ulnar avulsion	May have avulsion of ulna styloid Associated with injury to palmar and dorsal radio-ulnar ligaments. May result in instability
C. Distal avulsion	Distal avulsion of ulna lunate or ulna triquetral ligaments
D. Radial avulsion	Avulsion of insertion into radius, may be associated with a fracture

Fig. 41 Twenty-one-year male with pain persisting after a fall on the wrist some 6 weeks previously. Coronal T2* GE MR of wrist. There is a central perforation of the articular disc of the TFCC

intercarpal ligaments which occur in most carpal dislocations are not specifically identified and treated. Isolated soft tissue injuries do occur as a result of trauma. Rupture of the scapho-lunate ligament with rotary subluxation of the scaphoid has already been considered. The triangular fibrocartilage complex is another soft tissue structure which can be injured acutely. Bony injuries may be present, but in many cases it is an isolated soft tissue injury. Palmer (1989) classified injuries of the TFCC into acute traumatic (Palmer class 1) and chronic degenerative (Palmer class 2). It is only the former that will be considered here. Palmer further subclassified these acute TFCC injuries into 4 groups depending on the site of perforation (Table 2). MR has proven to be accurate in the assessment of TFCC injuries (Fig. 41) (Oneson et al. 1996), but MR arthrography may be required to detect these injuries (Zanetti et al. 2007). Imaging at higher field strength (3T) has been shown recently to improve identification of the injuries without the use of intra-articular contrast (Magee 2009).

6 Chronic/Overuse Injuries

Chronic stress injuries of the upper limb are far less common than in the lower limb. This is self-evident as in normal circumstances the upper limb is not weight bearing rending it much less likely to come under repetitive stress during normal daily activities. Stress injuries of the upper limb are thus almost exclusively found in those who undertake activities outwith the norm. Principally, this involves athletes' or those with unusual jobs that require use of the upper limb in an unusual activity.

In a review of 44 cases of upper limb stress injuries in athletes, SINHA et al. (1999) found only 17 occurred in the wrist. The only stress fractures reported involve the distal radius, the distal ulna and the scaphoid. Stress injuries in athletes may occur as a result of repetitive stresses applied at the site of muscular attachments to bone such as may occur with weight lifters. Alternatively, repeated weight bearing especially if there is impact loading can also result in a bony stress response. This has been described most often in gymnasts usually females as their routines include many activities (Webb and Rettig 2008), which involve weight bearing on the upper limb often with impact forces in addition. The radiology findings on plain films have been described (Carter et al. 1988). In a series of 8 gymnasts aged 14–16, radiographs of the wrist demonstrated irregularity and widening of the radial epipyhseal growth plate bilaterally but asymmetrically. The irregularity of the growth plate was largely marked on the metaphyseal side (Fig. 42). Some of the cases also showed an ill-defined cystic appearance. In 5 cases, the ulna growth plate was also affected but to a lesser extent. The findings have likened to the appearances seen in rickets (Liebling et al. 1995). The MR appearances have been described (Shih et al. 1995). In an

Fig. 42 AP radiograph of wrist of a young gymnast. There is widening of the epipyhseal plate with irregularity on the metaphyseal side

examination of 93 wrists in 47 gymnasts. The authors described several findings including widening of the growth plate, extension of the physeal cartilage into the metaphysis and or epiphysis. Also noted in some cases were vertical or horizontal fractures of the metaphysis. MR was more sensitive than plain films in the detection of most of these abnormalities. This has been confirmed in a recent paper (Dwek et al. 2009).

In addition to the metaphyseal stress injuries described above, the scaphoid has been reported to undergo stress fracture. Seven of Sinha's 44 cases had scaphoid stress fractures. These are seen in gymnasts but also in weight lifters. Weight bearing with the wrist in extension is the mechanism of injury which places repeated stress across the scaphoid waist. Stress fractures of the other carpal bones are exceptionally rare (Anderson 2006).

There are two further areas worth brief consideration. The first is the bone changes that may be seen within the wrist and carpus as a result of chronic vibration. Use of vibrating power tools such as pneumatic drills and chain saws may result in a spectrum of clinical disorders including white finger syndrome and carpal tunnel syndrome representing respectively vascular and neural changes as a result of exposure to repeated vibration over a long period of time. Furthermore, cystic changes visible on radiographs within the carpal bones particularly have been reported to occur in these workers. These changes in cysts measuring between 2 and 5 mm occur most commonly in the lunate and scaphoid. The association of these findings with occupational exposure is however inconsistent with some finding these changes almost as frequently within age-matched controls (Malchaire et al. 1986). There seems little evidence that those at risk should have regular screening radiographs of the wrists and in those with symptoms radiographic findings need to be treated with caution as cause and effect have not been proven (Gemne and Saraste 1987).

Finally, there are a few reports of instances of cysts developing at the site of healing fractures (Fig. 43). This is seen particularly in children with greenstick fractures, and the distal radius is the commonest site. The cystic change is seen initially at or close to the fracture site but persists and appears to migrate proximally into the diaphysis with time**.** On cross sectional imaging, the lesion is seen to lie not within the medullary cavity but in a juxtacortical or subperiosteal position (Roach et al. 2002). The pathogenesis is debated (Phillips and Keats 1986) with subperiosteal fat (Papadimitriou et al. 2005) subperiosteal (Durr et al. 1997) and intra-osseous haemorrhage all mooted as possible causes. The presence of a lucent lesion of bone away from the fracture site some time after the injury which may have healed can lead to diagnostic confusion with a tumour (Houshian et al. 2007) being considered as a possible cause. Thus, recognition of this entity with the typical cross-sectional appearance will prevent this erroneous diagnosis being entertained for too long.

7 Summary/Key Points

Careful evaluation of both AP and lateral radiographs is essential to avoid overlooking significant injury of the wrist and carpus. Understanding of ligamentous anatomy aids understanding of the injury patterns that occur.

Identification of one injury should alert one to the possibility of other associated injuries. Knowledge of the pattern of these injuries allows a systematic directed search to be undertaken.

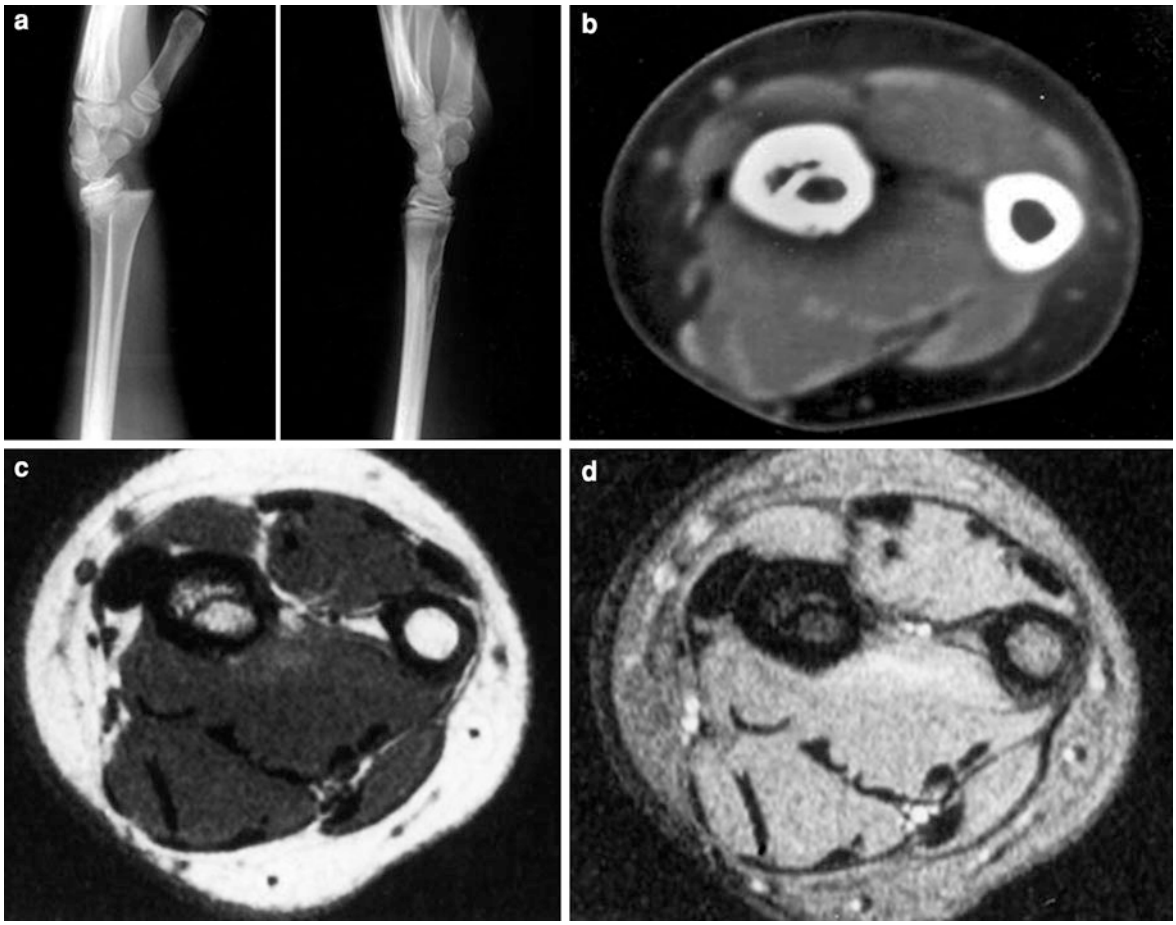

Fig. 43 **a** Lateral radiograph at time of injury demonstrating a Salter-Harris type 2 injury (left image) Later radiograph with fracture healed but cystic change evident on volar cortex (right image). **b** CT of lesion shows cystic area lies within cortex. **c** Axial T1- and **d** T2-weighted MR confirms fatty marrow content of lesion. Case reproduced with permission from reference 71

Lateral radiograph contains much vital information. It is essential to become familiar with its appearances and understand the normal anatomical relationships.

MR is a technique of choice for detecting occult scaphoid fractures.

Describe fractures and dislocations systematically rather than using eponymous names.

References

Adey L, Souer JS, Lozano-Calderon S, Palmer W, Lee SG, Ring D (2007) Computed tomography of suspected scaphoid fractures. J Hand Surg Am 32(1):61–66

Anderson MW (2006) Imaging of upper extremity stress fractures in the athlete. Clin Sports Med 25(3):489–504

Annamalai G, Raby N (2003) Scaphoid and pronator fat stripes are unreliable soft tissue signs in the detection of radiographically occult fractures. Clin Radiol 58(10):798–800

Barton JR (1838) Views and treatment of an important injury of the wrist. Med Exam 1:365–368

Barton NJ (1992) Twenty questions about scaphoid fractures. J Hand Surg[Br] 17B:289–310

Beeres FJ, Hogervorst M, Rhemrev SJ, den Hollander P, Jukema GN (2007) A prospective comparison for suspected scaphoid fractures: bone scintigraphy versus clinical outcome. Injury 38(7):769–774

Brøndum V, Larsen CF, Skov O (1992) Fracture of the carpal scaphoid: frequency and distribution in a well-defined population. Eur J Radiol 15(2):118–122

Brookes-Fazakerley SD, Kumar AJ, Oakley J (2009) Survey of the initial management and imaging protocols for occult scaphoid fractures in UK hospitals. Skeletal Radiol 38(11):1045–1048

Brydie A, Raby N (2003) Early MRI in the management of clinical scaphoid fracture. Br J Radiol 76(905):296–300

Carter SR, Aldridge MJ, Fitzgerald R, Davies AM (1988) Stress changes of the wrist in adolescent gymnasts. Br J Radiol 61(722):109–112

Cerezal L, Abascal F, Canga A, García-Valtuille R, Bustamante M, del Piñal F (2000) Usefulness of gadolinium-enhanced MR imaging in the evaluation of the vascularity of scaphoid nonunions. AJR Am J Roentgenol 174(1):141–149

Davidson JS, Brown DJ, Barnes SN, Bruce CE (2001) Simple treatment for torus fractures of the distal radius. J Bone Joint Surg (Br) 83-B:1173–1175

Dawson JS, Martel AL, Davis TR (2001) Scaphoid blood flow and acute fracture healing a dynamic MRI study with enhancement with gadolinium. J Bone Joint Surg [Br] 83-B:809–814

De Schrijver F, De Smet L (2001) Fracture of the hook of the hamate, often misdiagnosed as "wrist sprain". J Emerg Med 20(1):47–51

Dorsay TA, Major NM, Helms CA (2001) Cost-effectiveness of immediate MR imaging versus traditional follow-up for revealing radiographically occult scaphoid fractures. AJR 177:1257–1263

Dumontier C, Meyer zu Reckendorf G, Sautet A, Lenoble E, Saffar P, Allieu Y (2001) Radiocarpal dislocations: classification and proposal for treatment. A review of twenty-seven cases. J Bone Joint Surg Am 83-A(2):212–218

Duncan DS, Thurston AJ (1985) Clinical fracture of the scaphoid–an illusionary diagnosis. J Hand Surg 10B(3):375–376

Durr HR, Lienemann A, Stabler A, Kuehne J-H, Refior HJ (1997) MRI of posttraumatic cyst-like lesions of bone after a greenstick fracture. Eur Radiol 7:1218–1220

Dwek JR, Cardoso F, Chung CB (2009) MR imaging of overuse injuries in the skeletally immature gymnast: spectrum of soft-tissue and osseous lesions in the hand and wrist. Pediatr Radiol 39(12):1310–1316

Fernández DL (1993) Fractures of the distal radius: operative treatment. In: Heckman JD (ed) Instructional Course Lectures, vol 42. American Academy of Orthopaedic Surgeons, Park Ridge, pp 73–88

Fisher MR, Rogers LF, Hendrix RW (1983) Systematic approach to identifying fourth and fifth carpometacarpal joint dislocations. Am J Roentgenol 140(2):319–324

Foex B, Speake P, Body R (2005) Best evidence topic report. Magnetic resonance imaging or bone scintigraphy in the diagnosis of plain X-ray occult scaphoid fractures. Emerg Med J 22(6):434–435

Frykman G (1967) Fracture of the distal radius including sequelae-shoulder-hand-finger syndrome, disturbance in the distal radio-ulnar joint and impairment of nerve function. A clinical and experimental study. Acta Orthop Scand Suppl 108:3

Gaebler C (2006) Fractures and dislocations of the carpus. In: Buchholz RW, Heckmen JD, Court-Brown C (eds) Rockwood and green's fractures in adults, 6th edn. Lippincott Williams & Wilkins, Philadelphia, pp 857–908

Gemne G, Saraste H (1987) Bone and joint pathology in workers using hand-held vibrating tools. An overview. Scand J Work Environ Health 13(4):290–300

Gilula LA (1979) Carpal injuries: analytic approach and case exercises. Am J Roentgenol 133(3):503–517

Groves AM, Kayani I, Syed R, Hutton BF, Bearcroft PP, Dixon AK, Ell PJ (2006) An international survey of hospital practice in the imaging of acute scaphoid trauma. Am J Roentgenol 187(6):1453–1456

Houshian S, Pedersen NW, Torfing T, Venkatram N (2007) Post-traumatic cortical cysts in paediatric fractures: is it a concern for emergency doctors? A report of three cases. Eur J Emerg Med 14(6):365–367

Hudson TM, Caragol WJ, Kaye JJ (1976) Isolated rotatory subluxation of the carpal navicular. Am J Roentgenol 126(3):601–611

Ilyas A, Chaitanya C (2008) Radiocarpal fracture dislocations. J Am Acad Orthop Surg 16:647–655

Johnson RP (1980) The acutely injured wrist and its residuals. Clin Orthop 149:33–44

Jupiter JB, Fernandez DL (1997) Comparative classification for fractures of the distal end of the radius. J Hand Surg Am 22(4):563–571

Kaewlai R, Avery LL, Asrani AV, Abujudeh HH, Sacknoff R, Novelline RA (2008) Multidetector CT of carpal injuries: anatomy, fractures, and fracture-dislocations. Radiographics 28(6):1771–1784

Kato H, Nakamura R, Horii E, Nakao E, Yajima H (2000) Diagnostic imaging for fracture of the hook of the hamate. Hand Surg 5(1):19–24

Kumar S, O'Connor A, Despois M, Galloway H (2005) Use of early magnetic resonance imaging in the diagnosis of occult scaphoid fractures: the CAST Study. NZ Med J 118:1209

La Hei N, McFadyen I, Brock M, Field J (2007) Scaphoid bone bruising–probably not the precursor of asymptomatic non-union of the scaphoid. J Hand Surg Eur Vol 32(3):337–340

Leslie IJ, Dickson RA (1981) The fractured carpal scaphoid: natural history and factors influencing outcome. J Bone Joint Surg 63-B(2):225–230

Liebling MS, Berdon WE, Ruzal-Shapiro C, Levin TL, Roye D Jr, Wilkinson R (1995) Gymnast's wrist (pseudorickets growth plate abnormality) in adolescent athletes: findings on plain films and MR imaging. Am J Roentgenol 164(1):157–159

Lo IK, MacDermid JC, Bennett JD, Bogoch E, King GJ (2001) The radioulnar ratio: a new method of quantifying distal radioulnar joint subluxation. J Hand Surg Am 26(2):236–243

Low G, Raby N (2005) Can follow-up radiography for acute scaphoid fracture still be considered a valid investigation? Clin Radiol 60(10):1106–1110

Lozano-Calderón SA, Doornberg J, Ring D (2006) Fractures of the dorsal articular margin of the distal part of the radius with dorsal radiocarpal subluxation. J Bone Joint Surg Am 88:1486–1493

MacEwan DW (1964) Changes due to trauma in the fat plane overlying the pronator quadratus muscle: a radiologic sign. Radiology 82:879–881

Magee T (2009) Comparison of 3-T MRI and arthroscopy of intrinsic wrist ligament and TFCC tears. Am J Roentgenol 192(1):80–85

Malchaire J, Maldague B, Huberlant JM, Croquet F (1986) Bone and joint changes in the wrists and elbows and their association with hand and arm vibration exposure. Ann Occup Hyg 30(4):461–468

May MM, Lawton JN, Blazar PE (2002) Ulnar styloid fractures associated with distal radial fractures: incidence and implications for distal radioulnar joint instability. J Hand Surg [Am] 27(6):965–971

Melone CP (1986) Open treatment for displaced articular fractures of the distal radius. Clin Orthop 202:101–111

Memarsadeghi M, Breitenseher MJ, Schaefer-Prokop C, Weber M, Aldrian S, Gäbler C, Prokop M (2006) Occult scaphoid fractures: comparison of multidetector CT and MR imaging–initial experience. Radiology 240(1):169–176

Moneim MS, Bolger JT, Omer GE (1985) Radiocarpal dislocation–classification and rationale for management. Clin Orthop Relat Res 192:199–209

Nakamura R, Horii E, Imaeda T, Tsunoda K, Nakao E (1995) Distal radioulnar joint subluxation and dislocation diagnosed by standard roentgenography. Skeletal Radiol 24(2):91–94

Nakamura R, Horii E, Imaeda T, Nakao E (1996) Criteria for diagnosing distal radioulnar joint subluxation by computed tomography. Skeletal Radiol 25(7):649–653

Nicolaidis SC, Hildreth DH, Lichtman DM (2000) Acute injuries of the distal radioulnar joint. Hand Clin 16(3):449–459

Oneson SR, Scales LM, Timins ME, Erickson SJ, Chamoy L (1996) MR imaging interpretation of the Palmer classification of triangular fibrocartilage complex lesions. Radiographics 16(1):97–106

Palmer AK (1989) Triangular fibrocartilage complex lesions: a classification. J Hand Surg 14A:594–606

Papadimitriou NG, Christophorides J, Beslikas TA, Doulianaki EG, Papadimitriou AG (2005) Post-traumatic cystic lesion following fracture of the radius. Skeletal Radiol 34(7):411–414

Phillips CD, Keats TE (1986) The development of post-traumatic cyst-like lesions in bone. Skeletal Radiol 15:631–634

Raby N (2001) Magnetic resonance imaging of suspected scaphoid fractures using a low field dedicated extremity MR system. Clin Radiol 56(4):316–320

Raby N, Berman L, de Lacey G (2005) Accident and emergency radiology a survival guide, 2nd edn. Elsevier, Amsterdam

Roach RT, Cassar-Pullicino V, Summers BN (2002) Paediatric post-traumatic cortical defects of the distal radius. Pediatr Radiol 32(5):333–339

Rodgers LF (2001) Radiology of skeletal trauma, 3rd edn, Chap. 17. Churchill Livingstone, London

Shih C, Chang CY, Penn IW, Tiu CM, Chang T, Wu JJ (1995) Chronically stressed wrists in adolescent gymnasts: MR imaging appearance. Radiology 195:855–859

Singh AK, Davis TR, Dawson JS, Oni JA, Downing ND (2004) Gadolinium enhanced MR assessment of proximal fragment vascularity in nonunions after scaphoid fracture: does it predict the outcome of reconstructive surgery? J Hand Surg Br 29(5):444–448

Sinha AK, Kaeding CC, Wadley GM (1999) Upper extremity stress fractures in athletes: clinical features of 44 cases. Clin J Sport Med 9(4):199–202

Smith ML, Bain GI, Chabrel N, Turner P, Carter C, Field J (2009) Using computed tomography to assist with diagnosis of avascular necrosis complicating chronic scaphoid non-union. J Hand Surg Am 34(6):1037–1043

Thornton A, Gyll C (1999) Children's fractures. WB Saunders, London

Tiel-Van Buul MM, Van Beek EJ, Van Dongen A, Van Royen EA (1992a) The reliability of the 3 phase bone scan in suspected scaphoid fracture: an inter- and intra-observer variability analysis. Eur J Nucl Med 19:848–852

Tiel-Van Buul MMC, Van Beek EJR, Broekhuizen AH, Nooitgedacht EA, Davids PHP, Bakker AJ (1992b) Diagnosing scaphoid fractures: radiographs cannot be used as a gold standard. Injury 23(2):77–79

Tiel-Van Buul MN, Van Beek EJ, Born JJ, Gobler FN, Broekhuizen AH, Van Royen EA (1993) The value of radiographs and bone scintigraphy in suspected scaphoid fracture: a statistical analysis. J Hand Surg [Br] 18:403–406

Tsai P, Paksima N (2009) The distal radio ulnar joint. Bull NYU Hosp Jt Dis 67(1):90–96

Waizenegger M, Wastie ML, Barton NJ, Davis TRC (1994) Scintigraphy in the evaluation of the "clinical" scaphoid fracture. J Hand Surg [Br] 19B(6):750–753

Webb BG, Rettig LA (2008) Gymnastic wrist injuries. Curr Sports Med Rep 7(5):289–295

Yeager BA, Dalinka MK (1985) Radiology of trauma to the wrist: dislocations, fracture dislocations, and instability patterns. Skeletal Radiol 13(2):120–130

You JS, Chung SP, Chung HS, Park IC, Lee HS, Kim SH (2007) The usefulness of CT for patients with carpal bone fractures in the emergency department. Emerg Med J 24(4):248–250

Zanetti M, Saupe N, Nagy L (2007) Role of MR imaging in chronic wrist pain. Eur Radiol 17:927–938